Clinical Cancer Research

Antibody–Fc/FcR Interaction on Macrophages as a Mechanism for Hyperprogressive Disease in Non–small Cell Lung Cancer Subsequent to PD-1/PD-L1 Blockade

Giuseppe Lo Russo[1], Massimo Moro[2], Michele Sommariva[3], Valeria Cancila[4], Mattia Boeri[2], Giovanni Centonze[2], Simona Ferro[5], Monica Ganzinelli[1], Patrizia Gasparini[2], Veronica Huber[5], Massimo Milione[6], Luca Porcu[7], Claudia Proto[1], Giancarlo Pruneri[6,8], Diego Signorelli[1], Sabina Sangaletti[9], Lucia Sfondrini[3], Chiara Storti[3], Elena Tassi[10,11], Alberto Bardelli[12,13], Silvia Marsoni[12,14], Valter Torri[7], Claudio Tripodo[4], Mario Paolo Colombo[9], Andrea Anichini[10], Licia Rivoltini[5], Andrea Balsari[3], Gabriella Sozzi[2], and Marina Chiara Garassino[1]

Abstract

Purpose: Hyperprogression (HP), a paradoxical boost in tumor growth, was described in a subset of patients treated with immune checkpoint inhibitors (ICI). Neither clinicopathologic features nor biological mechanisms associated with HP have been identified.

Experimental Design: Among 187 patients with non–small cell lung cancer (NSCLC) treated with ICI at our institute, cases with HP were identified according to clinical and radiologic criteria. Baseline histologic samples from patients treated with ICI were evaluated by IHC for myeloid and lymphoid markers. T-cell–deficient mice, injected with human lung cancer cells and patient-derived xenografts (PDX) belonging to specific mutational subsets, were assessed for tumor growth after treatment with antibodies against mouse and human programmed death receptor-1 (PD-1). The immune microenvironment was evaluated by flow cytometry and IHC.

Results: Among 187 patients, 152 were evaluable for clinical response. We identified four categories: 32 cases were defined as responders (21%), 42 patients with stable disease (27.7%), 39 cases were defined as progressors (25.7%), and 39 patients with HP (25.7%). Pretreatment tissue samples from all patients with HP showed tumor infiltration by M2-like $CD163^+CD33^+PD\text{-}L1^+$ clustered epithelioid macrophages. Enrichment by tumor-associated macrophages (TAM) was observed, even in tumor nodules from immunodeficient mice injected with human lung cancer cells and with PDXs. In these models, tumor growth was enhanced by treatment with anti–PD-1 but not anti–PD-1 $F(ab)_2$ fragments.

Conclusions: These results suggest a crucial role of TAM reprogramming, upon Fc receptor engagement by ICI, eventually inducing HP and provide clues on a distinctive immunophenotype potentially able to predict HP.

See related commentary by Knorr and Ravetch, p. 904

Introduction

The advent of immune checkpoint inhibitors (ICI) has radically changed the paradigm of care for patients with non–small cell lung cancer (NSCLC). Several agents are now approved in the treatment of NSCLC on the basis of their superiority over chemotherapy (1, 2). Immunotherapy with antibodies targeting either the programmed death receptor 1 (PD-1) or its ligand (PD-L1) may provide long-term benefits in approximately 20% of patients (2). However, in a subset of patients, ICI paradoxically accelerates tumor growth, a phenomenon known as

[1]Medical Oncology Department 1, Fondazione IRCCS - Istituto Nazionale dei Tumori, Milan, Italy. [2]Department of Research, Fondazione IRCCS - Istituto Nazionale dei Tumori, Milan, Italy. [3]Department of Biomedical Sciences for Health, University of Milan, Milan, Italy. [4]Department of Health Sciences, Human Pathology Section, University of Palermo, Palermo, Italy. [5]Department of Research, Fondazione IRCCS - Istituto Nazionale dei Tumori, Milan, Italy. [6]Department of Pathology and Laboratory Medicine, Fondazione IRCCS - Istituto Nazionale dei Tumori, Milan, Italy. [7]Department of Oncology, IRCCS Istituto di Ricerche Farmacologiche Mario Negri, Milano, Italy. [8]Department of Oncology and Haematology, University of Milan, Milan, Italy. [9]Department of Research, Fondazione IRCCS - Istituto Nazionale dei Tumori, Milan, Italy. [10]Department of Research, Fondazione IRCCS - Istituto Nazionale dei Tumori, Milan, Italy. [11]Experimental Hematology Unit, IRCCS San Raffaele Scientific Institute, Milano, Italy. [12]Candiolo Cancer Institute-FPO, IRCCS, Candiolo, Italy. [13]Department of Oncology, University of Torino, Candiolo, Italy. [14]IFOM, Istituto Firc di Oncología Molecolare, Milan, Italy.

Note: Supplementary data for this article are available at Clinical Cancer Research Online (http://clincancerres.aacrjournals.org/).

G. Lo Russo, M. Moro, M. Sommariva, and V. Cancila contributed equally to this article.

A. Balsari, G. Sozzi, and M.C. Garassino share senior authorship.

Corresponding Author: Gabriella Sozzi, Fondazione IRCCS - Istituto Nazionale dei Tumori, Via Giacomo Venezian 1, Milan 20133, Italy. Phone: 3902-2390-2232; Fax: 3902-2390-2928; E-mail: gabriella.sozzi@istitutotumori.mi.it

doi: 10.1158/1078-0432.CCR-18-1390

Translational Relevance

Hyperprogressive disease in lung cancer and other tumors is an urgent clinical issue affecting 1 of 5 patients treated with immune checkpoint inhibitors (ICI), affecting their prognosis and leading to death in a very short time. As the use of immunotherapy increases in the clinic, it is important to understand the intricacies of this new treatment option to optimize treatment approaches. Data already published in the field mainly focused on adaptive immunity without finding any characteristics to predict *a priori* the phenomenon. Our preclinical findings underline the role of innate immunity in mediating hyperprogression (HP) via Fc/FcR triggering on macrophages by anti–PD-1 antibody. Accordingly, all patients with HP showed tumor infiltration by M2-like $CD163^{+}CD33^{+}PD\text{-}L1^{+}$ clustered epithelioid macrophages. These results, pointing to the involvement of innate immune cells in HP, provide new insights into the still unknown mechanisms behind a clinical conundrum.

hyperprogression (HP; refs. 3–6). Studies have estimated that the prevalence of HP in patients with different cancer histotypes treated with ICI may range between 9% and 29% (3–6). No significant histopathologic and molecular features capable of predicting *a priori* HP have been identified, with the partial exception of rare *MDM2* amplification and *EGFR* mutations (5). These observations have ignited an international debate regarding whether HP is a true phenomenon or only representative of a subset of patients with a particularly worse prognosis.

In the tumor microenvironment, the effector functions of innate immune cells may be blunted by the PD-1 receptor, as observed for T lymphocytes, suggesting that these innate cells are another potential target for ICI (7–9). Accordingly, it has been demonstrated that anti–PD-1 antibody can exert antitumor activity in immunodeficient mice via natural killer (NK) cells (8). Conversely, it has been demonstrated that, in $PD\text{-}1^{-/-}$ NK cells or in NK cells pretreated with anti–PD-1 antibody, the production of lytic molecules such as perforins and granzymes is decreased (10). Moreover, tumor-infiltrating dendritic cells (9) and monocytes (11) are reported to release the immunosuppressive cytokine IL10 upon anti–PD-1 treatment. Therefore, it is possible to hypothesize that in some circumstances, PD-1 blockade might exacerbate immunosuppression upon interaction with innate immune cells.

The aim of this study was to investigate, at the clinical and pathologic level, the phenomenon of HP in patients with NSCLC and to evaluate the role of innate immunity during ICI treatment. To eliminate the interference of T lymphocytes, we exploited cell lines and patient-derived xenografts (PDX) transplanted in immunodeficient mice.

Materials and Methods

Clinical series

Medical records, radiologic findings, and available tumor specimens were collected from patients with NSCLC treated with ICI at the Thoracic Unit of the Istituto Nazionale dei Tumori, Milan, Italy, from July 2013 to December 2017.The study complied with the Declaration of Helsinki and was done in accordance with good clinical practice guidelines. All samples were obtained according to the Internal Review and the Ethics Boards of the Istituto Nazionale Tumori of Milan and all patients provided informed consent. All experimental protocols were approved by the ethics boards of the Istituto Nazionale Tumori of Milan (Int 22/15). Radiologic evaluation (CT scan with or without brain MRI) was performed at treatment initiation and every 8 weeks thereafter. Considering that criteria to define patients with HP described by previous authors (3–6) are applicable only in advanced lines, our multidisciplinary team (oncologists, pneumologists, radiologists, and thoracic surgeons) created institutional clinical and radiologic criteria designed to identify patients with HP also in first-line treatment. Patients with HP or those patients defined as P were classified according to predefined criteria as follows: (i) time-to-treatment failure < 2 months (time-to-treatment failure is defined as the time from the start of treatment with ICI to ICI discontinuation for any reason, including progression, patient preference, toxicity, or death); (ii) increase of $\geq$50% in the sum of target lesions major diameters between baseline and first radiologic evaluation; (iii) appearance of at least two new lesions in an organ already involved between baseline and first radiologic evaluation; (iv) spread of the disease to a new organ between baseline and first radiologic evaluation; (v) clinical deterioration with decrease in Eastern Cooperative Oncology Group (ECOG) performance status $\geq$2 during the first 2 months of treatment.

Patients who fulfilled at least three of the clinical/radiologic criteria were defined as exhibiting HP, whereas patients with RECIST 1.1 progressive disease as best response without fulfilling at least three criteria were defined as P patients. All R patients and SD patients were classified according to their RECIST 1.1 best response. Only patients who underwent at least two cycles of ICI treatment were included in this analysis.

IHC

IHC was carried out on formalin-fixed paraffin-embedded (FFPE) human or PDX tissue sections as described in Supplementary Materials and Methods. All the slides were analyzed under a Zeiss Axioscope-A1 equipped with fluorescence module and microphotographs were collected using a Zeiss Axiocam 503 Color with the Zen 2.0 Software (Zeiss). All markers were scored according to the percentage of immunoreactive cells out of the total cellularity.

Animal studies

All xenograft experiments were undertaken using 8- to 9-week-old female athymic nude or SCID mice (Charles River Laboratories). Human NSCLC cell line H460 tumor-bearing athymic nude mice were treated intraperitoneally or peritumorally with either 200 μg of mAb anti-mouse PD-1 (clone RMP1-14, BioXCell) or saline, and with either peritumoral anti–PD-1 $F(ab)_2$ or isotype control. Experiments were carried out in groups of four SCID mice, bearing a PDX sample or a cell suspension (10^5 cells for H460 and PC9 xenograft experiments) in each flank. Mice were treated twice weekly with an intraperitoneal injection of 10 mg/kg nivolumab (Opdivo; Bristol-Myers Squibb) or nivolumab $F(ab)_2$ fragments. Mice were maintained in the Animal Facility of the Fondazione IRCCS Istituto Nazionale dei Tumori (Milan, Italy). Animal experiments were authorized by the Institutional Animal Welfare Body and the Italian Ministry of Health, and performed in accordance with national law (D.lgs 26/2014) and Guidelines for the Welfare of Animals in Experimental Neoplasia (12). At the end of each experiment, tumors were harvested for subsequent analyses.

Statistical analysis

Distribution of continuous and categorical biomarkers was summarized by the median as a measure of central tendency and absolute frequencies, respectively. The Cochran–Mantel–Haenszel χ^2 test was used to detect statistical association (i.e., $P < 0.05$) in univariate analysis. The median and interquartile range (IQR) follow-up was estimated using the reverse Kaplan–Meier method.

Results

Clinical and pathologic evidence in patients with advanced NSCLC treated with ICI

From July 2013 to December 2017, 187 patients with advanced NSCLC received treatment with ICI at the Thoracic Unit of the Medical Oncology Department at the Istituto Nazionale dei Tumori (Milan, Italy), and 152 patients were evaluable for response. We identified four categories: responders (R, 32 cases, 21%), patients with stable disease (SD, 42 cases, 27.7%), progressors (P, 39 cases, 25.7%), and patients with HP (39 cases, 25.7%). Patients' characteristics are described in Supplementary Table S1. In this population, after a median follow-up of 32.7 (IQR 15.1–39.6) months, 108 of 152 patients (71%) died. Median [95% confidence interval (CI)] overall survival (OS) in the overall population was 11.9 (95% CI, 8.8–15.5) months.

If we restrict the analysis to patients with HP, median OS significantly decreased to 4.4 (95% CI, 3.4–5.4) months as compared with 17.7 (95% CI, 13.4–24.1) in non-HP patients. Median OS was 8.7 (95% CI, 5.3–13.4), 17.7 (95% CI, 12.7–25.5), and not reached in P, SD, and R patients, respectively.

Supplementary Table S2 shows the differences between P and HP according to our criteria described in the Materials and Methods section. Of 187 patients, 64 were diagnosed in other centers and could not be included in the present histopathologic and molecular analysis. Of the remaining 123, 35 patients (11 with HP and 24 without HP) were evaluable for response and had tissue samples suitable for a wide IHC characterization and gene expression analysis. Patients' characteristics of the extensively analyzed 35 samples resemble the clinical characteristics of the whole treated population

IHC analysis was performed to assess the presence and distribution of tumor-infiltrating immune elements. The immunophenotype of 11 patients with HP was compared with that of 24 patients without HP (6 P, 11 SD, and 7 R). No significant differences were observed among all the clinical classes of patient with respect to the subsets of tumor-infiltrating T lymphocytes (TIL), evaluated by the density of $CD3^+$, $CD4^+$, and $CD8^+$ lymphocytes and $FOXP3^+$ regulatory T cells (Tregs). In addition, no differences were detected between classes of patient in the numbers of $CD138^+$ plasma cells (PC), $CD123^+$ plasmacytoid dendritic cells (pDC), peritumoral and stromal myeloperoxidase $(MPO)^+$ myeloid cells, $CD163^+$ macrophages, $CD33^+$, PD-1, and PD-$L1^+$ immune cells. However, MPO^+ myeloid cells within the tumor were directly correlated ($P = 0.0497$) and PD-L1 expression in tumor cells was inversely correlated ($P = 0.0457$) with HP. Furthermore, a statistical trend was shown for the M2 macrophage/myeloid-derived suppressor cells marker Arginase-A I (ArgI) on peritumoral immune cells ($P = 0.0666$; Supplementary Table S3).

Gene expression profile (GEP) analysis of pretreatment tumors did not show any relevant features except for underexpression of pathways related to proliferative activity and cell metabolism in patients experiencing HP after ICI (Supplementary Fig. S1A and S1B). The analyses of selected genes representative of immune subsets by qRT-PCR revealed overexpression of the *CD274* gene, encoding for PD-L1, as the only significant marker in R patients (Supplementary Fig. S1C). FISH of *MDM2* and *MDM4* genes, carried out on in a cohort of 30 FFPE NSCLC tissues derived from 11 patients with HP and 17 patients without HP, revealed the presence of 3 amplified tumors (2 *MDM2*, 1 *MDM4*) in patients with HP and 6 amplified tumors (4 *MDM2*, 1 *MDM4* and 1 *MDM2* and *MDM4*) in patients without HP (Supplementary Fig. S2).

Notably, we noticed that, in some cases, $CD163^+$ tumor-infiltrating macrophages showed epithelioid morphology (alveolar macrophage-like) with the tendency to form dense clusters within neoplastic foci (Fig. 1A). In these cases, the same cells were found to coexpress CD33 and PD-L1 (Figs. 1B and 2). Such a peculiar morphology, aggregation, and immunophenotype ($CD163^+CD33^+$PD-$L1^+$) of macrophages, which we define "complete immunophenotype," was observed in all patients with HP and found to be statistically significant versus patients without HP ($P < 0.0001$; Supplementary Tables S4 and S5). This complete immunophenotype was also observed in 1 P patient, 2 patients with SD, and 1 R patient (Supplementary Table S5). All other cases experiencing treatment response with stable or slowly progressive disease either lacked the presence of epithelioid macrophages or showed loose clustering, or lacked some of the above markers (mainly $CD33^-$ and/or PD-L1; Fig. 1C and D).

Anti-mouse PD-1 antibody induces tumor progression in athymic mice

Histopathologic analyses showed the presence of clustered $CD163^+CD33^+$PD-$L1^+$ epithelioid macrophages as a distinctive trait in tumors with HP. Therefore, we sought to test whether macrophages are involved in the detrimental effects associated with anti–PD-1 therapy in preclinical models. Athymic nude mice implanted with human H460 NSCLC cell line were treated either intraperitoneally (Fig. 3A) or peritumorally (Fig. 3B) with anti–PD-1 antibody (clone RMP1-14) or saline. Anti–PD-1 treatment increased tumor growth compared with the control group, regardless of route and schedule of treatment (Fig. 3A and B). Anti–PD-1 treatment was also associated with a significant increase in $CD45^+$ leukocyte infiltration at the host–tumor interface, evaluated by IHC (Fig. 3C). Such an increase was mainly due to increasing numbers of intratumoral macrophages ($F4/80^+$ cells) and Arginase-I^+–expressing cells, whereas the density of B lymphocytes ($CD45R/B220^+$), granulocytes ($Gr\text{-}1^+$), and NK ($NKp46^+$) cells was comparable with the control group (Fig. 3C). Of note, Arginase-I was also consistently expressed by the complete immunophenotype intratumor macrophages characterizing patients with HP (Fig. 1E). Tumor-associated macrophages (TAM) can express PD-1 and the blocking of this receptor restores antitumor functions (7). Thus, the detrimental boost in tumor growth may not be ascribed to such receptor blockade, but rather to the Fc domain of the antibody which is reported to modulate anti–PD-1 antibody functional activity (13). Accordingly, the same experiments were performed using anti–PD-1 $F(ab)_2$ fragments. The lack of the Fc portion abrogated the increase in tumor growth observed with the whole antibody (Fig. 3D).

Anti-human PD-1 antibody (nivolumab) induces tumor progression of PDXs in SCID mice

To exclude a direct involvement of PD-1 expression in immune cells, we treated SCID mice with anti-human PD-1 (nivolumab), which does not cross-react with the murine counterpart (Supplementary Fig. S3A). Because a link between HP and *EGFR* mutational status has been proposed by Kato and colleagues (5), we compared two NSCLC PDXs, with and without *EGFR* mutation:

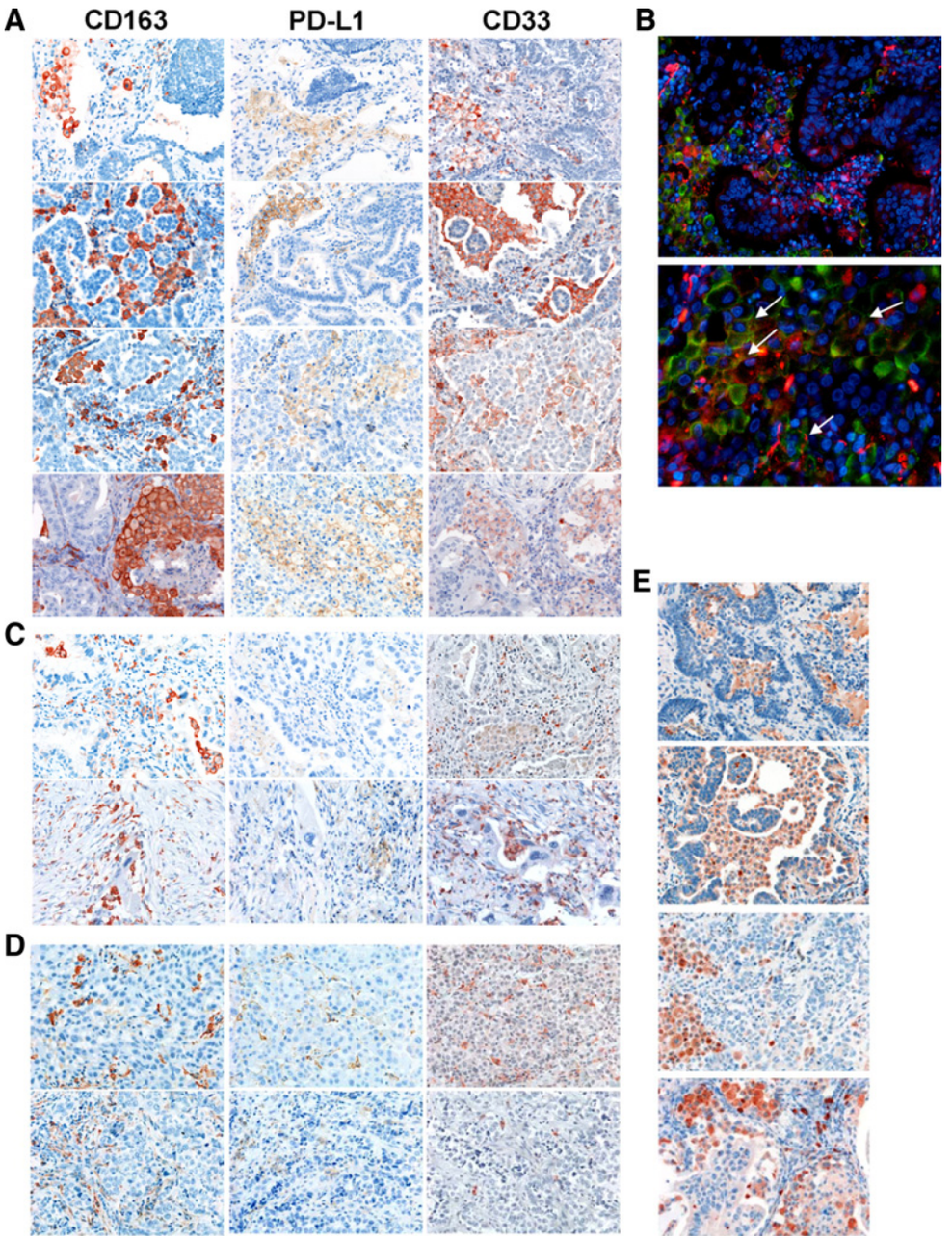

Figure 1.

IHC analyses for CD163, PD-L1, and CD33 in representative hyperprogressor and nonhyperprogressor cases. **A,** Representative microphotographs detailing the presence of macrophages displaying epithelioid morphology and expression of CD163, PD-L1, and CD33 markers (defined as complete phenotype) in 4 hyperprogressor cases. **B,** Double immunofluorescence staining for CD163 (green) and PD-L1 (red) showing the coexpression of the two markers in epithelioid macrophages (arrows). **C,** Representative microphotographs detailing the presence of macrophages displaying epithelioid morphology, variable clustering, and incomplete expression of the three CD163, PD-L1, and CD33 markers (defining the complete phenotype of HP patients) in 2 cases of non-HP patients (SD). **D,** Representative microphotographs detailing the presence of myeloid elements with nonepithelioid morphology (stellate or spindle-shaped cells) on CD163, PD-L1, and CD33 markers populating tumor infiltrates of non-HP patients (1 SD and 1 response). **E,** Representative microphotographs relative to Arginase-A1 expression by clustered epithelioid macrophages in 4 HP patients' infiltrates. Magnification 20×.

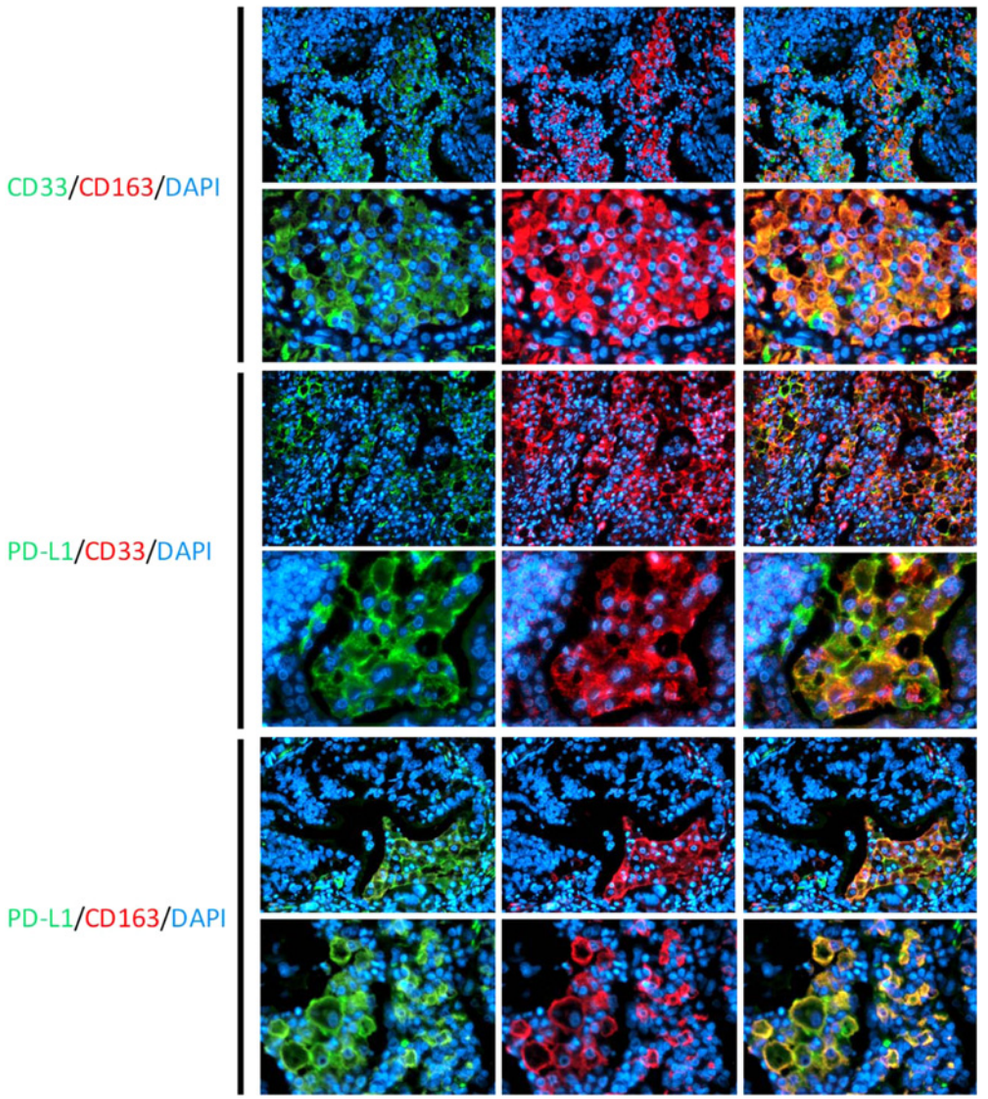

Figure 2.

Immunofluorescence panels from prototypical hyperprogressive disease infiltrates showing the colocalization of CD33, CD163, and PD-L1 in clustered macrophages with epithelioid morphology. Three different combinations of double-marker stainings are shown. Green signal and red signal correspond to Opal-520 and Opal-620 fluorophores, respectively. Original magnifications 100× and 400×.

PDX302 ($P53^{C135Y}$, $EGFR^{L858R}$, $KRAS^{WT}$, APC^{WT}) versus PDX305 ($P53^{WT}$, $EGFR^{WT}$, $KRAS^{G12C}$, APC^{R1114L}). On PDXs, before treatment, FACS analysis with human anti–PD-1 antibody showed expression of PD-1 receptor on a subset of tumor cells (around 1% $PD\text{-}1^+$ cells, Supplementary Fig. S3B). In addition, IHC analysis showed that $F4/80^+$ epithelioid/monocytoid elements, aggregated in clusters resembling those identified in patients with HP, were appreciable only in PDX302 (Supplementary Fig. S3C).

SCID mice carrying subcutaneous PDX302 ($n = 8$), but not PDX305 ($n = 8$), showed a significant increase in tumor growth rate compared with controls following twice weekly treatment with nivolumab (Fig. 4A). FACS analysis in lungs of PDX302 bearers showed increased cancer cell dissemination in nivolumab-treated mice but not in controls ($3.88 \pm 1.99\%$ vs. $0.87 \pm 0.33\%$, $P = 0.0286$, respectively; Fig. 4B), whereas no differences were detected in PDX305 bearers (data not shown).

FACS analysis was also performed on primary tumors for characterization of different myeloid subsets (CD11b, Ly6G, Ly6C, and F4/80) and NK cells (CD49b). In PDX302-bearing mice, an increase in $CD11b^+F4/80^{high}$ macrophages was observed in the nivolumab-treated group versus controls (Supplementary Fig. S3D), whereas no significant changes occurred in other immune subpopulations. Accordingly, IHC analysis performed on the same tumors revealed accumulation of macrophages and $ArgI^+$-expressing cells (Fig. 4C; Supplementary Fig. S3E). Notably, in PDX302, the $F4/80^+$ epithelioid/monocytoid clusters were enriched in nivolumab-treated tumors (Fig. 4C).

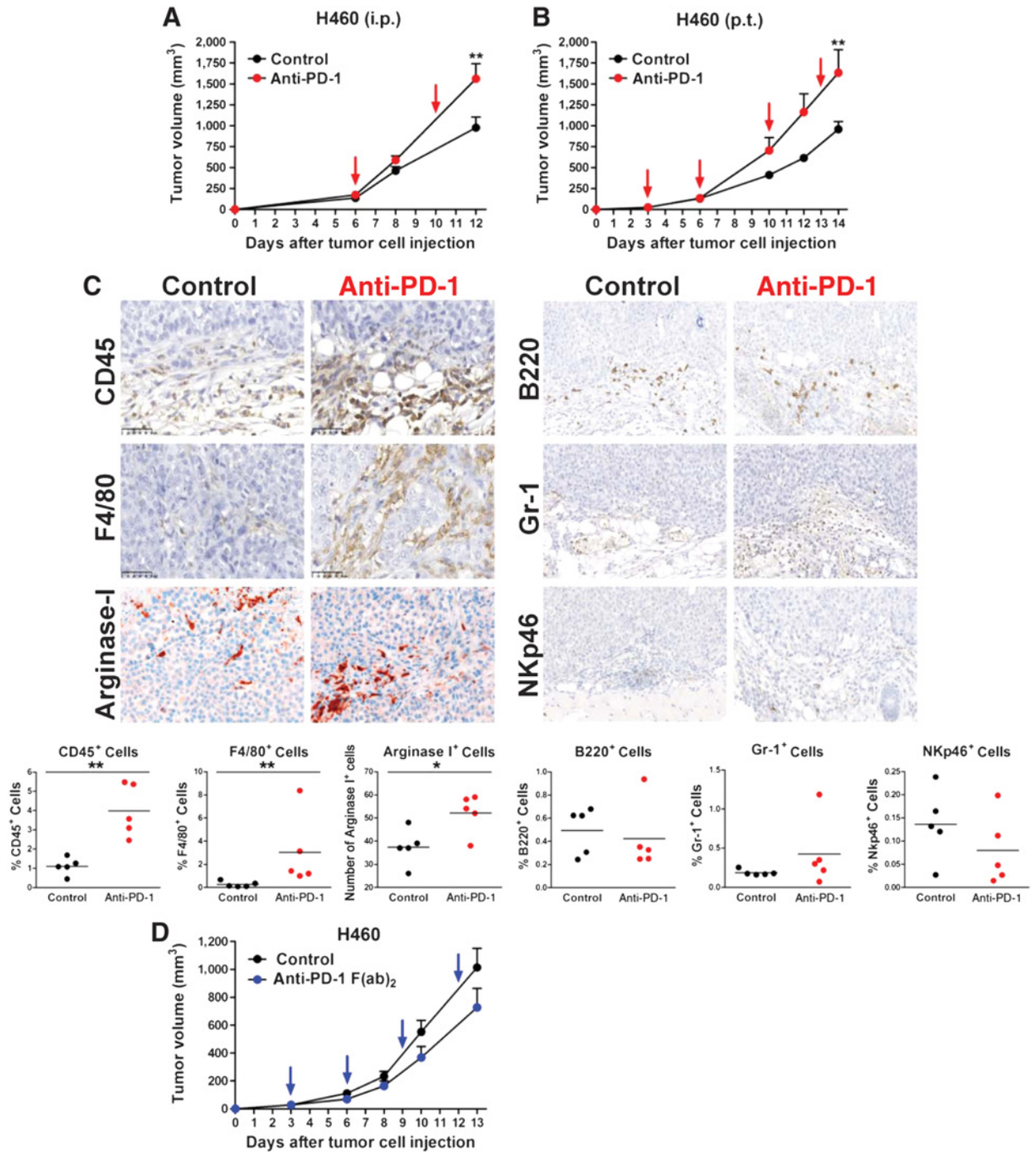

Figure 3.

Anti-mouse PD-1 antibody induces tumor progression in athymic mice. Athymic nude mice were xenografted with H460 lung cancer cell lines and treated intraperitoneally (i.p.; $n = 6$ mice/group; **A**) or peritumorally (p.t.; $n = 5$ mice/group; **B**) with 200 μg of anti-mouse PD-1 blocking antibody (red dots) or with vehicle (black dots). Red arrows indicate the days of anti–PD-1 antibody treatment. Dots represent mean ± SEM of tumor volume for each group. **, $P < 0.01$ by mixed models ANOVA. **C,** Representative IHC images and quantification of leukocytes ($CD45^+$), macrophages ($F4/80^+$), Arginase-I^+, B lymphocytes ($CD45R/B220^+$), granulocytes ($Gr\text{-}1^+$), and NK ($NKp46^+$) cells in the tumor microenvironment of H460 lung cancer xenografts collected from the study illustrated in Fig. 3B (peritumoral experiment; $n = 5$ mice/group). Original magnification 20×. *, $P < 0.05$; **, $P < 0.01$ by Mann–Whitney *U* test. **D,** Athymic nude mice were xenografted with H460 lung cancer cell lines and treated intraperitoneally with 200 μg anti–PD-1 $F(ab)_2$ (blue dots) or with vehicle (black dots; $n = 6$ mice/group). Blue arrows indicate the days of anti–PD-1 antibody treatment. Dots represent mean ± SEM of tumor volume for each group.

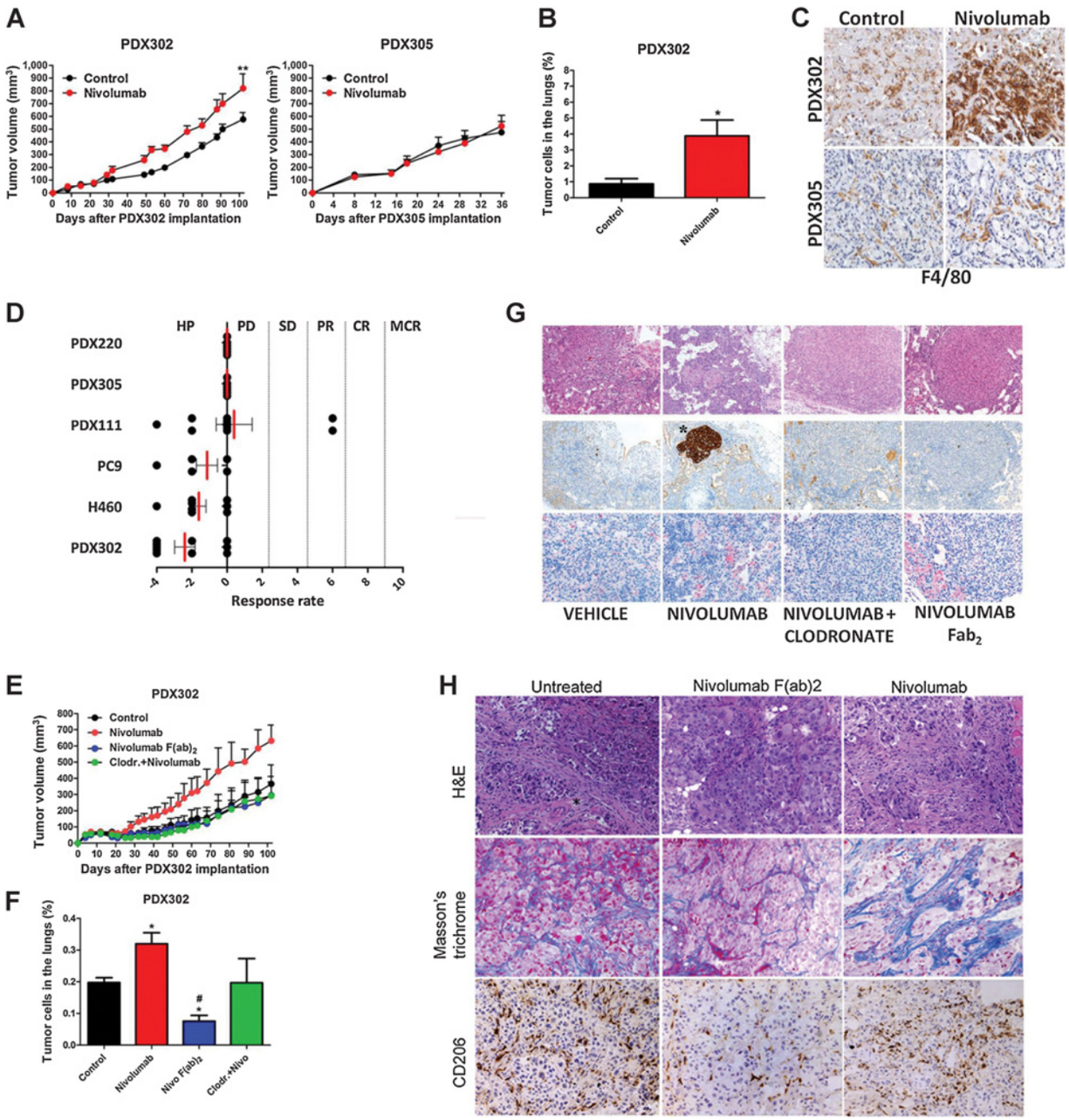

Figure 4.

Anti-human PD-1 antibody (nivolumab) induces tumor progression of PDXs in SCID mice. **A,** PDX302 (P53C135Y, EGFRL858R, KRASWT, APCWT) and PDX305 (P53WT, EGFRWT, KRASG13C, APCR1114L) samples were injected in both flanks of SCID mice ($n = 4$). Mice were treated with 10 mg/kg intraperitoneal nivolumab (red dots) twice weekly from day 1 after tumor implant to the end of the experiment. **, $P < 0.01$ by mixed models ANOVA. **B,** Analysis of tumor cells disseminated to mice lungs. Mice lungs were analyzed by FACS, after tissue dissociation to single cells, for the presence of human disseminated cells. Graphs indicate the percentage of human cells in nivolumab-treated and control mouse lungs. *, $P < 0.05$. **C,** Representative images showing F4/80$^+$ cells with epithelioid/monocytoid elements aggregated in clusters in an untreated PDX302 model. **D,** Dot plot summarizing the results of the effects of nivolumab treatment in all tested PDX (PDX302, PDX305, PDX111, and PDX220) and xenograft models (H460 and PC9). Response rate was estimated as described in the "Materials and Methods" section. CR, complete response; MCR, maintained complete response; PD, progressive disease; PR, partial response. **E,** PDX302 (P53C135Y, EGFRL858R, KRASWT, APCWT) samples were injected in both flanks of SCID mice ($n = 4$). Mice were treated with 10 mg/kg intraperitoneal nivolumab, nivolumab F(ab)2, or clodronate plus nivolumab twice weekly (once weekly for clodronate injection) from day 1 after tumor implant to the end of the experiment. *, $P < 0.05$. Clodr., clodronate. **F,** Analysis of tumor cells disseminated to mice lungs. Mice lungs were analyzed by FACS, after tissue dissociation to single cells, for the presence of human disseminated cells. Graphs indicate the percentage of human cells in nivolumab-, nivolumab F(ab)$_2$-, or clodronate plus nivolumab–treated and control mouse lungs. *, $P < 0.05$ compared with control; #$P < 0.05$ compared with nivolumab treated. Clodr., clodronate. **G,** Representative IHC images of mouse iliac lymph nodes showing tumor cell dissemination with the presence of a metastatic nodule (indicated by the asterisk) only in nivolumab-treated mice. CK, pan-cytokeratin staining; H&E, hematoxylin and eosin staining. **H,** Hematoxylin and eosin and Masson trichrome staining showing the presence of fibrotic areas with consistent matrix deposition in untreated, nivolumab-, and nivolumab F(ab)$_2$-treated representative cases. IHC analysis for CD206$^+$ macrophages highlighting the enrichment in macrophages in nivolumab-treated tumor.

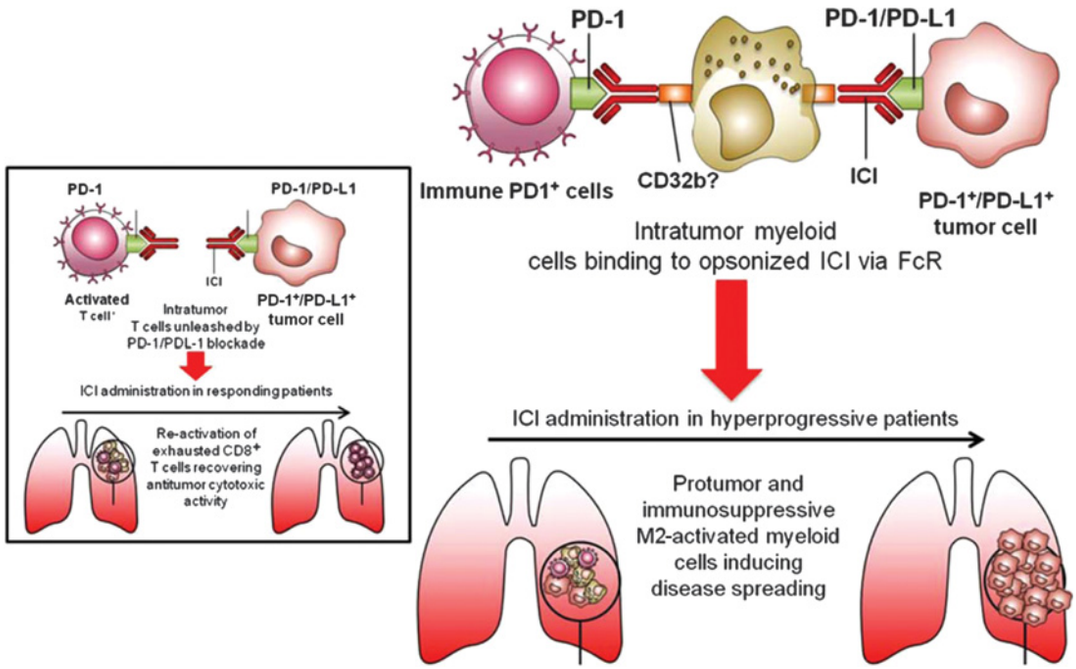

Figure 5.
Hypothesized mechanism through which macrophages and ICI are involved in determining HP.

Overall, these data indicate that in the *EGFR*-mutated PDX302-bearing mice, nivolumab triggers a detrimental effect characterized by increased tumor growth, lung dissemination, and the accrual of macrophages, most likely M2.

To further confirm the detrimental effect induced by nivolumab in other preclinical models, PDX111 ($P53^{C242X}$, $KRAS^{G12V}$, $CDKN2A^{E69X}$, $CTNNB1^{T41I}$), PDX220 (wild-type for all tested genes), H460 ($KRAS^{Q61H}$, $STK11^{Q37^*}$), and PC9 ($EGFR^{L858R}$, $EGFR^{E746\_A750del}$, $CDKN2A^{G67V}$) were xenografted in SCID mice. All tested models showed low levels of PD-1 expression on tumor cells (ranging from 0.6% to 4%, Supplementary Fig. S3B). As with PDX302, an increase in tumor growth was observed in H460- and PC9-bearing mice after nivolumab treatment. PDX111 tumors showed a variable response, whereas tumors in PDX220- and PDX305-bearing mice showed no response to nivolumab (Fig. 4D).

To reinforce the role of the Fc domain of the antibody in boosting tumor growth, PDX302-bearing SCID mice were treated with nivolumab-$F(ab)_2$ fragments. No HP-like growth was observed (Fig. 4E), whereas in the same experiment, mice treated with the entire antibody showed HP-like growth, dissemination to lung (Fig. 4F), and regional (iliac) lymph node metastases (Fig. 3G). In the group pretreated with clodronate, which reduces $F4/80^+$ macrophages, impaired nivolumab-induced tumor growth was observed (Fig. 4E). The $F4/80^+$ macrophages also stained for CD206 that marks M2-like subsets and aggregated in fibrotic-like areas in nivolumab-, but not in nivolumab $F(ab)_2$-treated tumors. In the latter, less fibrotic areas than in control mice were observed (Fig. 4H).

These results suggest that HP is sustained by nivolumab interaction with M2-like macrophages, most likely via Fc–Fcγ receptor binding (Fig. 5).

Discussion

Although ICI have changed the paradigm of care for patients with NSCLC, an in-depth examination of the Kaplan–Meier curves from the CheckMate-026 (14), CheckMate-057 (15), CheckMate-227 (16), and KEYNOTE-042 (17) trials showed an excess of disease progression and death in the immunotherapy treatment arms compared with chemotherapy in the first 3 months of treatment. This was also underscored by the European Medicines Agency in response to the appraisal for the second-line use of nivolumab in nonsquamous histologies (http://www.ema.europa.eu/docs/en_GB/document_library/EPAR_-_Product_Information/human/003985/WC500189765.pdf). Furthermore, the benefit of ICI in trials conducted in never smokers and in patients with *EGFR* mutation–positive or anaplastic lymphoma kinase (*ALK*) mutation–positive NSCLC seems unclear (1, 2, 5, 14, 15). The four most important articles on the HP topic showed prevalence rates ranging from 9% to 29% throughout tumor types, including NSCLC (3–6). In all these articles, the ratio of the tumor growth rates before and during ICI treatment was used to identify HP, although with slightly different cut-offs. None of these studies defined pathologic features able to predict HP, although *MDM2/4* amplification and *EGFR* alterations were proposed to be associated (5). However, we did not find any significant difference in the frequency of *MDM2/4* amplification between patients with and without HP, and the role of *EGFR* cannot be discussed due to the low number of *EGFR*-mutated patients included in our case series (Supplementary Table S1)

Our definition of HP is different from that used in the above-mentioned studies, where radiologic imaging before, at the start and after ICI is needed to identify HP. However, in clinical practice all these radiologic evaluations are often unavailable, and as a

consequence, the criteria used in literature are unable to classify patients with HP considering that ICI are starting to be widely used as first-line therapy. Furthermore, both RECIST 1.1 and Immune-related RECIST (irRECIST) criteria, used in the reported analyses, considered only changes in tumor size and did not take into account nontarget lesions, such as lymphangitis and pathologic lesions under 10 mm. In addition, functional and clinical aspects, such as deterioration in performance status, were not considered. Therefore, we decided to include both clinical and radiologic criteria to identify patients with HP in our series. These proposed criteria might overestimate the real fraction of patients experiencing HP; for these reasons, a clinical trial is ongoing within our Institute to properly validate the criteria and thereby obtain the true rate of HP as well as the distinctive immunophenotype.

Nivolumab-treated cell lines and PDX-bearing SCID mice mirrored the clinical observation of HP following treatment with ICI. Interestingly, patients and mice classified with HP share a similar tumor immunophenotype. Indeed, the population of $F4/80^+CD206^+$Arginase-$A1^+$ cells emerging from PDXs with HP matches macrophage features of the human counterpart (Figs. 1A, 4C, and 4H; and Supplementary Fig. S3C). M2-like macrophages were preferentially associated with fibrotic foci in PDXs that experience HP-like tumor growth after PD-1 blockade. The recruitment of these myeloid cells may promote a peculiar cancer-associated innate response that may affect tumor growth. Indeed, Knipper and colleagues. described a cross-talk between myeloid cells and fibroblasts promoting skin fibrosis that could provide proliferative and prosurvival signals in cancer cells (18). Prominent mitotic figures can be consistently identified in nivolumab-treated tumor foci embedded in a fibrotic stroma. In human samples, the accumulation of these cells is apparently unrelated to the extent and distribution of tumor-infiltrating T-cell populations.

The role of the innate immune system in mediating the effects of ICI is now clearly emerging. Cells of myeloid origin present in the tumor microenvironment decrease the effects of ICI via PD-L1 expression (19), by "stealing" anti–PD-1 antibody from the membrane of T lymphocytes that return to anergy (20) or by secreting immunosuppressive molecules (21). Our study provides novel evidence of negative immunoregulatory role exerted by $PD\text{-}L1^+$ macrophages enriched at tumor site under treatment with ICI. Pretreatment lesions from all patients classified as HP showed tumor infiltration by clustered epithelioid macrophages characterized by a $CD163^+CD33^+PD\text{-}L1^+$ profile. Interestingly, $CD163^+$ $PD\text{-}L1^+$ macrophages represent a common immune landscape for different tumors. $PD\text{-}L1^+$ macrophages have been recently described to accumulate in tight clusters at the tumor invasive margin in NSCLC (22). Macrophages expressing both PD-L1 and the "M2" marker CD163 have been described in MSI colorectal cancer (23), triple-negative breast cancer (24), gastric, and cervical cancer (25, 26). In some of these studies, the presence of $PD\text{-}L1^+$ macrophages has been associated with poor prognosis (24, 26) and/or with immunosuppressive function through IL10 production (27). In addition, the concurrent expression of CD163, CD33, and PD-L1 has been recently described in alveolar macrophages from patients with acute respiratory distress syndrome, a nononcologic condition present in 10% of subjects admitted to intensive care units (28). In this regard, we observed an increased infiltration of M2 macrophages after anti–PD-1 administration, providing evidence for their involvement in determining HP. TAMs can also express PD-1 that, if neutralized, can restore M1-like properties (7). This likely excludes blockade of PD-1 signaling in our models that remain rather oriented to M2. Therefore, we examined the possibility of FcR engagement as a modulator of anti–PD-1 activities (13). Upon testing the $F(ab)_2$ moiety in comparison with whole Ab, we have shown that nivolumab without the Fc domain no longer induces HP-like disease in our models.

The anti-mouse PD-1 clone RMP1-14, utilized for the treatment of tumor-bearing athymic mice, is a rat immunoglobulin IgG2a reported to interact with the mouse inhibitory receptor, FcγRIIb (13). FcγRIIb has been shown to be involved in dampening the immune response, and impairments in FcγRIIb function are associated with an exacerbation of inflammatory processes (29). The anti-human PD-1 antibody nivolumab is an IgG4 isotype with reduced binding affinity to activating FcγRs, thereby avoiding antibody-dependent cell-mediated cytotoxicity on $PD\text{-}1^+$ immune cells (30). However, nivolumab maintains the ability to bind to the inhibitory FcγRIIb receptor (13). Therefore, we suggest a possible role of FcγRIIb in the detrimental effect associated with anti–PD-1 therapy. However, since both human IgG4 and rat IgG2a can bind at lower affinity to other FcRs, the involvement of these receptors cannot be excluded. Furthermore, studies elucidating the involvement of FcRs in the development of HP are required. Very recently, a report described PD-1 expression in one NSCLC case with HP and in one mouse NSCLC cell line. The latter treated with anti-murine PD-1 Ab underwent accelerated tumor growth (31). This interesting and logical explanation of HP cannot be totally supported by the low expression/prevalence of PD-1 on tumors and by $F(ab)_2$ experiments in mice. We found clusters of PD-1–expressing cells in 2 of 11 patients with HP (data not shown) and in all xenografts and PDXs, although at low levels (0.6%–4%) and with no correlation with HP-like progression.

In conclusion, the ongoing debate regarding whether HP is a true phenomenon or only representative of patients with a particularly worse prognosis is confirmed in our preclinical models, where ICI are able to boost tumor growth in a manner akin to the clinical observations of HP in patients with NSCLC. Our results suggest that FcR triggering of clustered epithelioid macrophages with a specific immunophenotype by ICI delivers a signaling cascade that promotes functional reprogramming of these cells toward a more aggressive protumorigenic behavior. This eventually induces HP in a subset of patients with distinctive immune and genetic profiles (depicted in Fig. 5). Our analyses, for the first time, suggest a role of innate immunity in this process. A further prospective validation of the HP immunophenotype and its relationship with specific genotypes, as well as the new proposed clinical criteria to classify HP, is ongoing.

Disclosure of Potential Conflicts of Interest

D. Signorelli is a consultant/advisory board member for AstraZeneca. A. Anichini reports receiving commercial research grants from Bristol-Myers Squibb. M. Garassino reports receiving commercial research grants from MSD, speakers bureau honoraria from Bristol-Myers Squibb, MSD, Roche, and AstraZeneca, and is a consultant/advisory board member for Bristol-Myers Squibb, Roche, MSD, and AstraZeneca. No potential conflicts of interest were disclosed by the other authors.

Authors' Contributions

Conception and design: G. Lo Russo, M. Moro, V. Cancila, S. Marsoni, A. Anichini, L. Rivoltini, A. Balsari, G. Sozzi, M.C. Garassino

Development of methodology: G. Lo Russo, M. Moro, G. Centonze, P. Gasparini, M. Milione, L. Porcu, C. Storti, A. Anichini, M.C. Garassino
Acquisition of data (provided animals, acquired and managed patients, provided facilities, etc.): G. Lo Russo, M. Moro, M. Sommariva, M. Ganzinelli, C. Proto, G. Pruneri, D. Signorelli, S. Sangaletti, L. Sfondrini, E. Tassi, G. Sozzi, M.C. Garassino
Analysis and interpretation of data (e.g., statistical analysis, biostatistics, computational analysis): G. Lo Russo, M. Sommariva, V. Cancila, M. Boeri, S. Ferro, M. Ganzinelli, V. Huber, M. Milione, L. Porcu, C. Proto, G. Pruneri, D. Signorelli, L. Sfondrini, E. Tassi, A. Bardelli, V. Torri, C. Tripodo, M.P. Colombo, A. Anichini, G. Sozzi, M.C. Garassino
Writing, review, and/or revision of the manuscript: G. Lo Russo, M. Moro, M. Sommariva, M. Ganzinelli, C. Proto, G. Pruneri, D. Signorelli, E. Tassi, A. Bardelli, S. Marsoni, V. Torri, C. Tripodo, M.P. Colombo, A. Anichini, A. Balsari, G. Sozzi, M.C. Garassino
Administrative, technical, or material support (i.e., reporting or organizing data, constructing databases): G. Lo Russo, M. Boeri, C. Proto, D. Signorelli, M.C. Garassino
Study supervision: G. Lo Russo, S. Marsoni, L. Rivoltini, G. Sozzi, M.C. Garassino

Acknowledgments

The authors wish to thank the following individuals: Dr. M. Figini for the production of nivolumab-F(ab)$_2$, Dr. L. De Cecco for GEP profiles, Dr. M. Dugo for bioinformatic analyses, Mrs. A. Cova and Dr. A. Berzi for technical assistance, Dr. A. Martinetti for biological sample collection, Dr. E. Tagliabue for data discussion and interpretation, Dr. G. Morello for her precious support in performing double-marker immunolocalization analyses, and Dr. G. Apolone for continuous support in the planning and execution of the study and for scientific writing. The authors would also like to acknowledge the editorial assistance provided by Chris Cammack, a professional medical writer at Ashfield Healthcare Communications, an Ashfield Company, part of UDG Healthcare plc. This work was supported by the Italian Ministry of Health (5×1000 Funds – 2014, to M.C. Garassino; grant no. GR-2013-02355637, to S. Sangaletti), AIRC (Associazione Italiana per la Ricerca sul Cancro; grant no.15190, to A. Balsari; grant no. 18812, to G. Sozzi; grant no. 17431, to A. Anichini; grant no. 10137, to M.P. Colombo), and EU project Horizon2020-686089 - PRECIOUS (to L. Rivoltini). E. Tassi was supported by a fellowship from Fondazione Beretta-Berlucchi.

The costs of publication of this article were defrayed in part by the payment of page charges. This article must therefore be hereby marked *advertisement* in accordance with 18 U.S.C. Section 1734 solely to indicate this fact.

Received May 4, 2018; revised July 25, 2018; accepted September 6, 2018; published first September 11, 2018.

References

1. Califano R, Kerr K, Morgan RD, Lo Russo G, Garassino M, Morgillo F, et al. Immune checkpoint blockade: a new era for non-small cell lung cancer. Curr Oncol Rep 2016;18:59.
2. Assi HI, Kamphorst AO, Moukalled NM, Ramalingam SS. Immune checkpoint inhibitors in advanced non–small cell lung cancer. Cancer 2018; 124:248–61.
3. Champiat S, Dercle L, Ammari S, Massard C, Hollebecque A, Postel-Vinay S, et al. Hyperprogressive disease is a new pattern of progression in cancer patients treated by anti-PD-1/PD-L1. Clin Cancer Res 2017;23:1920–8.
4. Saâda-Bouzid E, Defaucheux C, Karabajakian A, Coloma VP, Servois V, Paoletti X, et al. Hyperprogression during anti-PD-1/PD-L1 therapy in patients with recurrent and/or metastatic head and neck squamous cell carcinoma. Ann Oncol 2017;28:1605–11.
5. Kato S, Goodman A, Walavalkar V, Barkauskas DA, Sharabi A, Kurzrock R. Hyperprogressors after immunotherapy: analysis of genomic alterations associated with accelerated growth rate. Clin Cancer Res 2017; 23:4242–50.
6. Ferrara R, Caramella C, Texier M, Valette CA, Tessonnier L, Mezquita L, et al. Hyperprogressive disease (HPD) is frequent in non-small cell lung cancer (NSCLC) patients (pts) treated with anti PD1/PD-L1 monoclonal antibodies (IO). Ann Oncol 2017;28:abstract 1306PD.
7. Gordon SR, Maute RL, Dulken BW, Hutter G, George BM, McCracken MN, et al. PD-1 expression by tumour-associated macrophages inhibits phagocytosis and tumour immunity. Nature 2017;545:495–9.
8. Liu Y, Cheng Y, Xu Y, Wang Z, Du X, Li C, et al. Increased expression of programmed cell death protein 1 on NK cells inhibits NK-cell-mediated anti-tumor function and indicates poor prognosis in digestive cancers. Oncogene 2017;36:6143–53.
9. Lamichhane P, Karyampudi L, Shreeder B, Krempski J, Bahr D, Daum J, et al. IL10 release upon PD-1 blockade sustains immunosuppression in ovarian cancer. Cancer Res 2017;77:6667–78.
10. Solaymani-Mohammadi S, Lakhdari O, Minev I, Shenouda S, Frey BF, Billeskov R, et al. Lack of the programmed death-1 receptor renders host susceptible to enteric microbial infection through impairing the production of the mucosal natural killer cell effector molecules. J Leukoc Biol 2015 2015;99:2–9.
11. Said EA, Dupuy FP, Trautmann L, Zhang Y, Shi Y, El-Far M, et al. Programmed death-1-induced interleukin-10 production by monocytes impairs CD4 + T cell activation during HIV infection. Nat Med 2010; 16:452–9.
12. Workman P, Aboagye EO, Balkwill F, Balmain A, Bruder G, Chaplin DJ, et al. Guidelines for the welfare and use of animals in cancer research. Br J Cancer 2010;102:1555–77.
13. Dahan R, Sega E, Engelhardt J, Selby M, Korman AJ, Ravetch J V. FcγRs modulate the anti-tumor activity of antibodies targeting the PD-1/PD-L1 axis. Cancer Cell 2015;28:285–95.
14. Carbone DP, Reck M, Paz-Ares L, Creelan B, Horn L, Steins M, et al. First-line nivolumab in stage IV or recurrent non–small-cell lung cancer. N Engl J Med 2017;376:2415–26.
15. Borghaei H, Paz-Ares L, Horn L, Spigel DR, Steins M, Ready NE, et al. Nivolumab versus docetaxel in advanced nonsquamous non–small-cell lung cancer. N Engl J Med 2015;373:1627–39.
16. Hellmann MD, Ciuleanu T-E, Pluzanski A, Lee JS, Otterson GA, Audigier-Valette C, et al. Nivolumab plus ipilimumab in Llng cancer with a high tumor mutational burden. N Engl J Med 2018;378:2093-2104.
17. Lopes G, Wu Y-L, Kudaba I, Kowalski D, Chul Cho B, Castro G, et al. Pembrolizumab (pembro) versus platinum-based chemotherapy (chemo) as first-line therapy for advanced/metastatic NSCLC with a PD-L1 tumor proportion score (TPS) $\geq$ 1%: open-label, phase 3 KEYNOTE-042 study. J Clin Oncol 36s, 2018 (suppl; abstr LBA4).
18. Knipper JA, Willenborg S, Brinckmann J, Bloch W, Maaß T, Wagener R, et al. Interleukin-4 receptor α signaling in myeloid cells controls collagen fibril assembly in skin repair. Immunity 2015;43:803–16.
19. Antonios JP, Soto H, Everson RG, Moughon D, Orpilla JR, Shin NP, et al. Immunosuppressive tumor-infltrating myeloid cells mediate adaptive immune resistance via a PD-1/PD-L1 mechanism in glioblastoma. Neuro Oncol 2017;19:796–807.
20. Arlauckas SP, Garris CS, Kohler RH, Kitaoka M, Cuccarese MF, Yang KS, et al. *In vivo* imaging reveals a tumor-associated macrophage – mediated resistance pathway in anti – PD-1 therapy. Sci Transl Med 2017;1–10.
21. Marvel D, Gabrilovich DI. Myeloid-derived suppressor cells in the tumor microenvironment: expect the unexpected. J Clin Investig 2015; 125:3356–64.
22. Lavin Y, Kobayashi S, Leader A, Amir ED, Elefant N, Bigenwald C, et al. Innate immune landscape in early lung adenocarcinoma by paired single-cell analyses. Cell 2017;169:750–765.
23. Korehisa S, Oki E, Iimori M, Nakaji Y, Shimokawa M, Saeki H, et al. Clinical significance of programmed cell death-ligand 1 expression and the immune microenvironment at the invasive front of colorectal cancers with high microsatellite instability. Int J Cancer 2018;142:822–32.
24. Adams A, Vail P, Ruiz A, Mollaee M, McCue P, Knudsen E, et al. Composite analysis of immunological and metabolic markers defines novel subtypes of triple negative breast cancer. Mod Pathol 2018;2:288–98.

25. Harada K, Dong X, Estrella JS, Correa AM, Xu Y, Hofstetter WL, et al. Tumor-associated macrophage infiltration is highly associated with PD-L1 expression in gastric adenocarcinoma. Gastric Cancer 2018; 21:31–40.
26. Heeren AM, Punt S, Bleeker MC, Gaarenstroom KN, Van Der Velden J, Kenter GG, et al. Prognostic effect of different PD-L1 expression patterns in squamous cell carcinoma and adenocarcinoma of the cervix. Mod Pathol 2016;29:753–63.
27. Kubota K, Moriyama M, Furukawa S, Rafiul HASM, Maruse Y, Jinno T, et al. CD163+CD204+ tumor-associated macrophages contribute to T cell regulation via interleukin-10 and PD-L1 production in oral squamous cell carcinoma. Sci Rep 2017;7:1–12.
28. Morrell ED, Wiedeman A, Long SA, Gharib SA, West TE, Skerrett SJ, et al. Cytometry TOF identifies alveolar macrophage subtypes in acute respiratory distress syndrome. JCI Insight 2018;3:1–11.
29. Roghanian A, Stopforth RJ, Dahal LN, Cragg MS. New revelations from an old receptor: immunoregulatory functions of the inhibitory Fc gamma receptor, FcγRIIB (CD32B). J Leukoc Biol 2018 Feb 6 [Epub ahead of print].
30. Madorsky Rowdo FP, Baron A, Urrutia M, Mordoh J. Immunotherapy in cancer: A combat between tumors and the immune system; you win some, you lose some. Front Immunol 2015;6:2–13.
31. Du S, McCall N, Park K, Guan Q, Fontina P, Ertel A, et al. Blockade of tumor-expressed PD-1 promotes lung cancer growth. Oncoimmunology 2018;7: e1408747.